# Bilateral Adaptive Control of Nonlinear Teleoperation Systems with Uncertain Dynamics and Dead-zone

**Xia Liu**
School of Electrical Engineering and Electronic Information, Xihua University
Chengdu, Sichuan 610039, China
e-mail: xliu_uestc@yahoo.com

**Mahdi Tavakoli**
Department of Electrical and Computer Engineering, University of Alberta
Edmonton, Alberta T6G 2V4, Canada
e-mail: mahdi.tavakoli@ualberta.ca

**Abstract:** Dead-zone is one of the most common hard nonlinearities ubiquitous in master-slave teleoperation systems, particularly in the slave robot joints. However, adaptive control techniques applied in teleoperation systems usually deal with dynamic uncertainty but ignore the presence of dead-zone. Dead-zone has the potential to remarkably deteriorate the transparency of a teleoperation system in the sense of position and force tracking performance or even destabilizing the system if not compensated for in the control scheme. In this paper, an adaptive bilateral control scheme is proposed for nonlinear teleoperation systems in the presence of both uncertain dynamics and dead-zone. An adaptive controller is designed for the master robot with dynamic uncertainties and another is developed for the slave robot with both dynamic uncertainties and unknown dead-zone. The two controllers are incorporated into the 4-channel bilateral teleoperation control framework to achieve transparency. The transparency and stability of the closed-loop teleoperation system is studied via a Lyapunov function analysis. Comparisons with the conventional adaptive control which merely deal with dynamic uncertainties in the simulations demonstrate the validity of the proposed approach.

**Keywords:** Bilateral teleoperation systems, dead-zone, dynamic uncertainties, adaptive control, transparency

## 1 INTRODUCTION

A general teleoperation system consists of a slave robot that can reach and interact with its environment, and a master robot from which the human operator applies his/her desired commands to the slave robot. If force feedback from the slave to the master is presented through communication channel, then the teleoperation system is said to be bilateral. Teleoperation systems have been widely applied to areas such as nuclear waste handling, undersea and outer space explorations, remote-based rehabilitation, minimally invasive surgery and so on [1].

Transparency is a critical requirement for a teleoperation system, requiring the slave to accurately follow the position of the master while the operator faithfully feels the contact force being applied from the slave to the environment. In practice, however, there are uncertainties in teleoperation systems that degrade the system transparency and undermine its stability. An effective way to deal with these difficulties is to apply adaptive control schemes in which the controllers adjust to compensate for these uncertainties. For this case, Zhu [2] developed an adaptive control approach for nonlinear teleoperation systems with parameter uncertainties where the model of the human operator and the environment were incorporated into the dynamics of the master and the slave. Hung [3] designed an adaptive controller for nonlinear teleoperation systems where the dynamic parameters of the master and the slave were not accurate. Chopra [4] presented an adaptive control scheme for nonlinear teleoperators with uncertain physical parameters as well as time-delay. Nuño [5] extended Chopra's scheme and proposed an improved adaptive controller to remove the limitation on gravity forces of the master and the slave. A control scheme is proposed for bilateral teleoperation systems subject to

saturation in actuators in [6]. Adaptive controllers were designed for bilateral teleoperation systems with uncertain dynamics and kinematics, or linearly and nonlinearly parameterized dynamic uncertainties by the authors in [7]. In recent years, Islam [8] proposed a nonlinear adaptive scheme with local proportional and derivative signals to cope with parametric dynamic uncertainty for teleoperation systems with symmetrical and unsymmetrical time-varying delay. Zhai [9] developed an adaptive control approach based on switched filter for teleoperation system with varying time-varying delays and with actuator saturation. Franco [10] presented a discrete-time adaptive-predictive control algorithm for a teleoperation system with force disturbance and input delay. Wang [11] developed an adaptive neural control approach based on radial basis functions neural networks for bilateral teleoperation systems with time delay and backlash-like hysteresis. Abut [12] employed adaptive computed torque control for teleoperation systems to cope with the kinematic and dynamic uncertainties and the interaction forces between the operator and the environment. Li [13] proposed an adaptive control framework for teleoperation systems with dynamic and kinematic uncertainties and time-varying time delays to achieve master-slave synchronization in the task space. Lu [14] proposed an adaptive fuzzy control strategy based on linear matrix inequalities for bimanual teleoperation system to evaluate and suppress the contact forces and dynamic uncertainties. Nevertheless, all of the above control schemes neglect dead-zone in a teleoperation system.

Dead-zone is one of the most common hard nonlinearities in master-slave teleoperation systems, particularly in the slave robot joints. The slave robot usually has actuated revolute joints. The active joints of the slave robot are actuated by electric

servomotors. Consequently, dead-zone is ubiquitous in the actuators of the slave robot. Dead-zone is particularly harmful and it has the potential to cause oscillations and inaccuracy, remarkably undermining the system transparency or even destabilizing the system if not compensated for in the control scheme. It should be noted that for the master robot it is typically designed with care to involve no or little dead-zone so that the sensation of reflected forces by the human operator is realistic.

Outside the realm of teleoperation systems, adaptive control is also an important research trust to mitigate the effect of dead-zone in nonlinear systems; this was pioneered by Tao [15]. Roughly speaking, the main idea underlying this approach is to construct an inverse model of the dead-zone and update it adaptively. However, as pointed in [16] "the requirement on dead-zone inversion may cause amplification of additive measurement disturbances resulting from the inversion". In order to avoid introducing the dead-zone inverse, Wang [17] proposed a robust adaptive control scheme for nonlinear dynamic systems preceded by an unknown dead-zone. However, in [17] only motion control is focused on for a class of SISO (Single-Input, Single-Output) nonlinear systems rather than force control. It is worth noting that in a nonlinear bilateral teleoperation system which is MIMO (Multi-Input, Multi-Output), force feedback is a requisite besides motion control. So far, there has been no attempt at simultaneous motion and force control of a master-slave bilateral teleoperation system with unknown dead-zone.

This paper presents an adaptive scheme able to deal with nonlinear bilateral teleoperation systems in the presence of both dynamic uncertainties and dead-zone. A controller is designed for the master with dynamic uncertainties and another is developed for the slave with simultaneous intrinsic dynamic uncertainties and unknown dead-zone.

Then, the two adaptive controllers are incorporated into the 4-channel bilateral teleoperation control framework to achieve transparency in the sense of good position and force tracking performance. The proposed adaptive control scheme not only achieves transparency but also ensures stability of the system when exact knowledge of the dynamics and dead-zone is unavailable.

The rest of this paper is organized as follows. In Section 2, the model of nonlinear teleoperation systems with uncertain dynamics and dead-zone is presented. An adaptive control scheme that can simultaneously deal with dynamic uncertainties and dead-zone is designed in Section 3. In Section 4, the stability and transparency of the system is mathematically proved. In Section 5, simulations are conducted to demonstrate the validity of the proposed approach. The paper is concluded in Section 6.

## 2 MODEL OF NONLINEAR TELEOPERATION SYSTEMS WITH UNCERTAIN DYNAMICS AND DEAD-ZONE

In this section the model of teleoperation system is given. Also, the uncertainties in the dynamics and dead-zone are analyzed.

### 2.1 Dynamics of the Master and the Slave

The joint-space models of *n*-DOF master and the slave robots can be written as [18]:

$$\mathbf{M}_m(\mathbf{q}_m)\ddot{\mathbf{q}}_m + \mathbf{C}_m(\mathbf{q}_m,\dot{\mathbf{q}}_m)\dot{\mathbf{q}}_m + \mathbf{G}_m(\mathbf{q}_m) = \boldsymbol{\tau}_m + \boldsymbol{\tau}_h \tag{1}$$

$$\mathbf{M}_s(\mathbf{q}_s)\ddot{\mathbf{q}}_s + \mathbf{C}_s(\mathbf{q}_s,\dot{\mathbf{q}}_s)\dot{\mathbf{q}}_s + \mathbf{G}_s(\mathbf{q}_s) = \boldsymbol{\tau}_s - \boldsymbol{\tau}_e \tag{2}$$

where $\mathbf{q}_m$ and $\mathbf{q}_s \in \Re^{n\times 1}$ are joint positions, $\mathbf{M}_m(\mathbf{q}_m)$ and $\mathbf{M}_s(\mathbf{q}_s) \in \Re^{n\times n}$ are symmetric positive-definite inertia matrices, $\mathbf{C}_m(\mathbf{q}_m,\dot{\mathbf{q}}_m)$ and $\mathbf{C}_s(\mathbf{q}_s,\dot{\mathbf{q}}_s) \in \Re^{n\times n}$ correspond to Coriolis and centrifugal terms, $\mathbf{G}_m(\mathbf{q}_m)$ and $\mathbf{G}_s(\mathbf{q}_s) \in \Re^{n\times 1}$ represent gravity terms, $\boldsymbol{\tau}_m$

and $\boldsymbol{\tau}_s \in \Re^{n\times 1}$ are control torque inputs for the master and the slave, respectively. Here, $\boldsymbol{\tau}_h \in \Re^{n\times 1}$ is the torque applied from the operator to the master and $\boldsymbol{\tau}_e \in \Re^{n\times 1}$ is the torque applied from the slave to the environment. The subscripts $m$ and $s$ for the master and the slave, respectively, are omitted in the following important properties.

**Property 1 [3].** The terms in the left-hand sides of (1) and (2) can be expressed in a linear form with respect a set of constant dynamic parameters as:

$$\mathbf{M}(\mathbf{q})\ddot{\mathbf{q}} + \mathbf{C}(\mathbf{q},\dot{\mathbf{q}})\dot{\mathbf{q}} + \mathbf{G}(\mathbf{q}) = \mathbf{Y}(\mathbf{q},\dot{\mathbf{q}},\ddot{\mathbf{q}})\boldsymbol{\theta}$$

where $\mathbf{Y}(\mathbf{q},\dot{\mathbf{q}},\ddot{\mathbf{q}}) \in \Re^{n\times p}$ is called the dynamic regressor matrix and it is a known nonlinear matrix function with respect to the joint variables, and $\boldsymbol{\theta} \in \Re^{p\times 1}$ is a possibly unknown vector which consists of constant dynamic parameters $\theta_1, \theta_2, ..., \theta_p$, i.e., $\boldsymbol{\theta} = [\theta_1, \theta_2, ..., \theta_p]^T$.

Alternatively, Property 1 can also be described in another form as Property 1' in the following form.

**Property 1' [3]**. Each term in the left-hand sides of (1) and (2) can be expressed in a linear form with respect a set of constant dynamic parameters as:

$$\mathbf{M}(\mathbf{q})\ddot{\mathbf{q}} = \mathbf{Y}_0(\mathbf{q},\dot{\mathbf{q}},\ddot{\mathbf{q}})\boldsymbol{\theta}$$

$$\mathbf{C}(\mathbf{q},\dot{\mathbf{q}})\dot{\mathbf{q}} = \mathbf{Y}_1(\mathbf{q},\dot{\mathbf{q}})\boldsymbol{\theta}$$

$$\mathbf{G}(\mathbf{q}) = \mathbf{Y}_2(\mathbf{q})\boldsymbol{\theta}$$

where $\mathbf{Y}_0(\mathbf{q},\dot{\mathbf{q}},\ddot{\mathbf{q}})$, $\mathbf{Y}_1(\mathbf{q},\dot{\mathbf{q}})$, $\mathbf{Y}_2(\mathbf{q}) \in \Re^{n\times p}$ are dynamic regressor matrices and $\mathbf{Y}_1(\mathbf{q},\dot{\mathbf{q}},\ddot{\mathbf{q}}) + \mathbf{Y}_2(\mathbf{q},\dot{\mathbf{q}}) + \mathbf{Y}_3(\mathbf{q}) = \mathbf{Y}(\mathbf{q},\dot{\mathbf{q}},\ddot{\mathbf{q}})$.

**Property 2 [3].** The matrix $\dot{\mathbf{M}}(\mathbf{q}) - 2\mathbf{C}(\mathbf{q},\dot{\mathbf{q}})$ is skew-symmetric, i.e.,

$$\zeta^T(\dot{\mathbf{M}}(\mathbf{q}) - 2\mathbf{C}(\mathbf{q},\dot{\mathbf{q}}))\boldsymbol{\xi} = 0, \forall \boldsymbol{\xi} \in \Re^{n\times 1}.$$

## 2.2 Analysis of the Dead-Zone

Dead-zone is a static input-output relationship, which causes the output to be zero for a range of input values. In a teleoperation system, the slave robot often suffers from dead-zone imperfection. For instance, the dead-zone in the actuators of the slave joints can create a position error between the master robot and the slave robot. A typically graphical representation of the dead-zone at the input of the slave robot is shown in Fig. 1, where $i$ ( $i = 1, 2, ..., n$ ) denotes the $i$ th joint of the slave robot, $v_i(t)$ and $DZ_i(v_i(t))$ are the input and output of the dead-zone, respectively, $b_{r_i}$ and $b_{l_i}$ are break-points, and $m_{r_i}$ and $m_{l_i}$ are slopes.

A well assessed dead-zone, capturing most of its characteristics, is described using piecewise linear functions as [15]:

$$DZ_i(v_i(t)) = \begin{cases} m_{r_i}(v_i(t) - b_{r_i}) & if \quad v_i(t) \geq b_{r_i} \\ 0 & if \quad b_l < v_i(t) < b_{r_i} \\ m_{l_i}(v_i(t) - b_{l_i}) & if \quad v_i(t) \leq b_{l_i} \end{cases} \tag{3}$$

Generally, the dead-zone model is uncertain and its parameters $b_{r_i}$ , $b_{l_i}$ , $m_{r_i}$ and $m_{l_i}$ are unknown. However, it is assumed in this paper that $b_{r_i}$ , $b_{l_i}$ , $m_{r_i}$ and $m_{l_i}$ are bounded and their signs are usually known. This assumption has been successfully adopted in [17]. Therefore, it is not unreasonable to let $b_{r_i} > 0$ , $b_{l_i} < 0$ , $m_{r_i} > 0$ , $m_{l_i} > 0$ thereafter in this paper. Furthermore, it is assumed in this paper that $m_{r_i} = m_{l_i} = m$ . Such an assumption has been successfully adopted in the past [19].

Conventionally, the main idea of combating dead-zone is to construct an inverse model. However, possible amplification of additive measurement disturbances may result from the inverse model. In this paper, the dead-zone model (3) is redefined as follows to avoid constructing the dead-zone inverse.

$$DZ_i(v_i(t)) = mv_i(t) + dz_i(v_i(t)) \tag{4}$$

where

$$dz_i(v_i(t)) = \begin{cases} -mb_{r_i} & if \quad v_i(t) \geq b_{r_i} \\ -mv_i(t) & if \quad b_{l_i} < v_i(t) < b_{r_i} \\ -mb_{l_i} & if \quad v_i(t) \leq b_{l_i} \end{cases} \tag{5}$$

As aforementioned, $m_{r_i} = m_{l_i} = m$ and the parameters $b_{r_i}$, $b_{l_i}$, $m_{r_i}$ and $m_{l_i}$ are bounded, therefore, it is not difficult to get that $dz_i(v_i(t))$ is also bounded, i.e., $|dz_i(v_i(t))| \leq \alpha$, where $\alpha > 0$ is the known upper-bound of $dz_i(v_i(t))$.

### 2.3 Analysis of the Dynamic Uncertainties

As for the master robot, we consider the dynamic parameters are uncertain, i.e., $\boldsymbol{\theta}_m$ is uncertain. Then, according to Property 1, the left side of the dynamics of the master robot (1) can be rewritten as:

$$\hat{\mathbf{M}}_m(\mathbf{q}_m)\ddot{\mathbf{q}}_m + \hat{\mathbf{C}}_m(\mathbf{q}_m, \dot{\mathbf{q}}_m)\dot{\mathbf{q}}_m + \hat{\mathbf{G}}_m(\mathbf{q}_m) = \mathbf{Y}_m(\mathbf{q}_m, \dot{\mathbf{q}}_m, \ddot{\mathbf{q}}_m)\hat{\boldsymbol{\theta}}_m \tag{6}$$

where $\hat{\boldsymbol{\theta}}_m$ is the estimate of the unknown dynamic parameter vector $\boldsymbol{\theta}_m$ and $\mathbf{Y}_m(\mathbf{q}_m, \dot{\mathbf{q}}_m, \ddot{\mathbf{q}}_m)$ is the known dynamic regressor matrix of the master.

On the other hand, as for the slave robot, we consider the dynamic parameter vector $\boldsymbol{\theta}_{s*}$ is uncertain. Moreover, the dead-zone in the slave robot is unknown, i.e., the dead-zone parameter $m$ is unknown. Then, according to Property 1, the left side of the dynamics of the slave robot (2) can be rewritten as:

$$\hat{\mathbf{M}}_s(\mathbf{q}_s)\ddot{\mathbf{q}}_s + \hat{\mathbf{C}}_s(\mathbf{q}_s, \dot{\mathbf{q}}_s)\dot{\mathbf{q}}_s + \hat{\mathbf{G}}_s(\mathbf{q}_s) = \hat{\mathbf{M}}_s(\mathbf{q}_s)\ddot{\mathbf{q}}_s + \mathbf{Y}_{s1}(\mathbf{q}_s, \dot{\mathbf{q}}_s)\hat{\boldsymbol{\theta}}_{s*} + \mathbf{Y}_{s2}(\mathbf{q}_s)\hat{\boldsymbol{\theta}}_{s*} \tag{7}$$

where $\hat{\boldsymbol{\theta}}_{s*}$ is the estimate of the unknown dynamic parameter vector $\boldsymbol{\theta}_{s*}$ and $\mathbf{Y}_{s1}(\mathbf{q}_s, \dot{\mathbf{q}}_s)$, $\mathbf{Y}_{s2}(\mathbf{q}_s)$ are the known dynamic regressor matrices of the slave. Thereafter, $\mathbf{Y}_m(\mathbf{q}_m, \dot{\mathbf{q}}_m, \ddot{\mathbf{q}}_m)$, $\mathbf{Y}_{s1}(\mathbf{q}_s, \dot{\mathbf{q}}_s)$ and $\mathbf{Y}_{s2}(\mathbf{q}_s)$ will be denoted as $\mathbf{Y}_m$, $\mathbf{Y}_{s1}$ and $\mathbf{Y}_{s2}$ for brevity.

## 3. DESIGN OF 4-CHANNEL ADAPTIVE TELEOPERATION CONTROLLERS

The main idea pursued in this paper is to synthesize adaptive controllers able to account for the presence of the dynamic uncertainties in the master, and the simultaneous dynamic uncertainties and unknown dead-zone in the slave. Then the two controllers are incorporated into the 4-channel bilateral teleoperation control framework to achieve transparency.

### 3.1 Architecture of the Proposed 4-Channel Adaptive Teleoperation Control

For achieving transparency in a bilateral teleoperation system, various control architectures such as the PEB (Position Error Based), DFR (Direct Force Reflection) and 4-channel have been proposed. Among them, the 4-channel architecture is the most general case (it can represent the PEB and DFR through appropriate selection of controllers) and one that can achieve perfect transparency. More detailed proof of the transparency of 4-channel architecture can be found in [20].

Considering the dynamic uncertainties in the master and the slave, and the unknown dead-zone included in the slave, the architecture of the proposed control scheme is shown in Fig. 2. As it can be seen, the fixed (i.e. non-adaptive) position controller for the master (blocks $\mathbf{C}_L$ and $\mathbf{C}_4$) in the original 4-channel [21] are replaced by an adaptive position controller for the master to deal with dynamic uncertainties, and the fixed position controller for the slave (blocks $\mathbf{C}_R$ and $\mathbf{C}_1$) in the original 4-channel

are replaced by another adaptive position controller for the slave to deal with both dynamic uncertainties and unknown dead-zone. In the proposed approach blocks $\mathbf{C}_2$ and $\mathbf{C}_3$ are force feedback terms, and $\mathbf{C}_5$ and $\mathbf{C}_6$ are local force feedback. Besides, the signals $\boldsymbol{\tau}_h^*$ and $\boldsymbol{\tau}_e^*$ denote the exogenous torques of the operator and the environment, respectively.

### 3.2 Design of Control Laws and Adaptation Laws for the Master and the Slave

The adaptive controller for the master is designed to account for the dynamic uncertainties in the nonlinear model of the robot. First, define a virtual velocity error vector for the master:

$$\mathbf{s}_m = \Delta\dot{\mathbf{q}}_m + \boldsymbol{\Lambda}_m \Delta\mathbf{q}_m = \dot{\mathbf{q}}_m - \dot{\mathbf{q}}_{mr} \tag{8}$$

where $\Delta\mathbf{q}_m = \mathbf{q}_m - \mathbf{q}_s$, $\dot{\mathbf{q}}_{mr} = \dot{\mathbf{q}}_s - \boldsymbol{\Lambda}_m \Delta\mathbf{q}_m$ and $\boldsymbol{\Lambda}_m \in \Re^{n\times n}$ is a diagonal positive-definite constant matrix. From (8), we can get:

$$\dot{\mathbf{q}}_m = \mathbf{s}_m + \dot{\mathbf{q}}_{mr}, \quad \ddot{\mathbf{q}}_m = \dot{\mathbf{s}}_m + \ddot{\mathbf{q}}_{mr} \tag{9}$$

Substituting (9) into (1) and using Property 1, the open-loop dynamics of the master becomes:

$$\mathbf{M}_m(\mathbf{q}_m)\dot{\mathbf{s}}_m + \mathbf{C}_m(\mathbf{q}_m, \dot{\mathbf{q}}_m)\mathbf{s}_m = \boldsymbol{\tau}_m + \boldsymbol{\tau}_h - \mathbf{Y}_{mr}(\mathbf{q}_m, \dot{\mathbf{q}}_m, \dot{\mathbf{q}}_{mr}, \ddot{\mathbf{q}}_{mr})\boldsymbol{\theta}_m \tag{10}$$

where $\mathbf{Y}_{mr}(\mathbf{q}_m, \dot{\mathbf{q}}_m, \dot{\mathbf{q}}_{mr}, \ddot{\mathbf{q}}_{mr})\boldsymbol{\theta}_m = \mathbf{M}_m(\mathbf{q}_m)\ddot{\mathbf{q}}_{mr} + \mathbf{C}_m(\mathbf{q}_m, \dot{\mathbf{q}}_m)\dot{\mathbf{q}}_{mr} + \mathbf{G}_m(\mathbf{q}_m)$.

Thus the control law and the adaptation law for the master can be designed as follows.

● ***Control law for the master:***

$$\boldsymbol{\tau}_m = -\mathbf{K}_m\mathbf{s}_m + \mathbf{Y}_{mr}\hat{\boldsymbol{\theta}}_m + C_2(\boldsymbol{\tau}_h - \boldsymbol{\tau}_e) - \boldsymbol{\tau}_h \tag{11}$$

where $\mathbf{K}_m \in \Re^{n\times n}$ is a diagonal positive-definite constant matrix and $C_2$ is a positive constant.

● ***Dynamic adaptation law for the master:***

$$\dot{\hat{\boldsymbol{\theta}}}_m = -\boldsymbol{\Gamma}_m \mathbf{Y}_{mr}^T \mathbf{s}_m \tag{12}$$

where $\boldsymbol{\Gamma}_m \in \Re^{p\times p}$ is a diagonal positive-definite constant matrix and $p$ is the number of the elements that the dynamic parameter vector $\boldsymbol{\theta}_m$ includes as mentioned in Property 1.

The control law for the master (11) includes four terms. The first term is a feedback law involving the velocity and position tracking errors between the master and the slave, and the second term compensates for the dynamic uncertainties. These first two terms together perform adaptive position control for the master (as shown in the upper dashed box in Fig. 2). The third term implements force tracking between the master and the slave, and the fourth term is the local force feedback at the master side which is fed to the master controller. The estimate $\hat{\boldsymbol{\theta}}_m$ is updated by the dynamic adaptation law in (12). Substituting the control law (11) into (10), the closed-loop equation for the master is obtained as:

$$\mathbf{M}_m(\mathbf{q}_m)\dot{\mathbf{s}}_m + \mathbf{C}_m(\mathbf{q}_m,\dot{\mathbf{q}}_m)\mathbf{s}_m = -\mathbf{K}_m\mathbf{s}_m + \mathbf{Y}_{mr}\Delta\boldsymbol{\theta}_m + C_2(\boldsymbol{\tau}_h - \boldsymbol{\tau}_e) \tag{13}$$

where $\Delta\boldsymbol{\theta}_m = \hat{\boldsymbol{\theta}}_m - \boldsymbol{\theta}_m$.

Another adaptive controller is developed for the slave with unknown dead-zone in addition to the intrinsically uncertain dynamics. By choosing $\mathbf{q}_s$ and $\dot{\mathbf{q}}_s$ as the states, we obtain the state vector of the slave as $\mathbf{x}_s = [\mathbf{q}_s;\dot{\mathbf{q}}_s] \in \Re^{2n\times 1}$. For the slave, the desired position is the position trajectory of the master $\mathbf{x}_m = [\mathbf{q}_m;\dot{\mathbf{q}}_m] \in \Re^{2n\times 1}$. Now define a virtual sliding velocity error vector for the slave:

$$\mathbf{s}_s = \mathbf{\Lambda}_{ts}\Delta\mathbf{x}_s \tag{14}$$

where $\Delta\mathbf{x}_s = \mathbf{x}_s - \mathbf{x}_m$ and $\mathbf{\Lambda}_{ts} \in \Re^{n\times 2n}$ is a constant positive matrix.

Differentiating both sides of (14), we have:

$$\dot{\mathbf{s}}_s = \mathbf{\Lambda}_s\Delta\mathbf{x}_s + \ddot{\mathbf{q}}_s - \ddot{\mathbf{q}}_m \tag{15}$$

where $\mathbf{\Lambda}_s \in \Re^{n\times 2n}$ is a constant positive matrix satisfying $\mathbf{\Lambda}_{ts}\Delta\dot{\mathbf{x}}_s(t) = \mathbf{\Lambda}_s\Delta\mathbf{x}_s + \ddot{\mathbf{q}}_s - \ddot{\mathbf{q}}_m$.

In order not to directly use the virtual sliding velocity error $\mathbf{s}_s$ in the adaptation law which may cause chattering, a new virtual velocity error variable $\mathbf{s}_\varepsilon$ is introduced:

$$\mathbf{s}_\varepsilon = \mathbf{s}_s - \varepsilon sat(\frac{\mathbf{s}_s}{\varepsilon}) \tag{16}$$

where $\varepsilon$ is an arbitrary positive constant and $sat(.)$ is the saturation function defined as:

$$sat(\frac{s_{s_i}}{\varepsilon}) = \begin{cases} 1 & if \quad s_{s_i} > \varepsilon \\ -1 & if \quad s_{s_i} < -\varepsilon \\ \dfrac{s_{s_i}}{\varepsilon} & if \quad -\varepsilon \le s_{s_i} \le \varepsilon \end{cases} \tag{17}$$

where $i = 1,...,n$ and $\mathbf{s}_s = [s_{s_1}, s_{s_2}, ..., s_{s_n}]$. Here, it is not unreasonable to assume that $\left\|\dot{\mathbf{M}}_s(\mathbf{q}_s)\mathbf{s}_\varepsilon\right\| \le \beta$, where $\beta > 0$ is a constant.

Substituting (15) into (2) and using Property 1, the open-loop of the slave becomes:

$$\begin{aligned} &\mathbf{M}_s(\mathbf{q}_s)\dot{\mathbf{s}}_s - \mathbf{M}_s(\mathbf{q}_s)\mathbf{\Lambda}_s\Delta\mathbf{x}_s + \mathbf{M}_s(\mathbf{q}_s)\ddot{\mathbf{q}}_m + \mathbf{Y}_{s1}\boldsymbol{\theta}_{s*} + \mathbf{Y}_{s2}\boldsymbol{\theta}_{s*} \\ &= \boldsymbol{\tau}_s - \boldsymbol{\tau}_e \end{aligned} \tag{18}$$

Before introducing the control law for the slave, some definitions are needed:

$$\phi = \frac{1}{m},$$

$$\mathbf{E}_s = \ddot{\mathbf{q}}_m - \mathbf{\Lambda}_s \Delta \mathbf{x}_s \in \Re^{n\times 1},$$

$$\mathbf{Y}_s = \mathbf{Y}_{s1} + \mathbf{Y}_{s2} \in \Re^{n\times p},$$

$$\boldsymbol{\theta}_s = \frac{1}{m}\boldsymbol{\theta}_{s*} \in \Re^{p\times 1}.$$

We can now introduce the adaptive control law for the slave robot.

● ***Control law for the slave:***

$$\boldsymbol{\tau}_s = m\mathbf{v}(t) + dz(\mathbf{v}(t)) + \boldsymbol{\tau}_e + C_3(\boldsymbol{\tau}_h - \boldsymbol{\tau}_e) \tag{19}$$

$$\mathbf{v}(t) = -\mathbf{K}_s\mathbf{s}_s + \hat{\phi}\mathbf{E}_s + \mathbf{Y}_s\hat{\boldsymbol{\theta}}_s - \mathbf{K}_s^* sat(\frac{\mathbf{s}_s}{\varepsilon}) \tag{20}$$

where $\mathbf{v}(t) = [v_1(t), v_2(t), ..., v_n(t)]^T$, $dz(\mathbf{v}(t)) = [dz_1(v_1(t)), dz_2(v_2(t)), ..., dz_n(v_n(t))]^T$, and $C_3$ is a positive constant. Also, $\mathbf{K}_s \in \Re^{n\times n}$ is a diagonal positive-definite constant matrix, $\mathbf{K}_s^* \in \Re^{n\times n}$ is a positive-definite matrix which satisfies $eig_{\min}(\mathbf{K}_s\varepsilon + \mathbf{K}_s^*) \geq \frac{\alpha}{m} + \frac{\beta}{2m}$, where $eig_{\min}(\mathbf{K}_s\varepsilon + \mathbf{K}_s^*)$ is the minimum eigenvalue of $\mathbf{K}_s\varepsilon + \mathbf{K}_s^*$ and $\alpha, \beta > 0$ have been defined before. Besides, $\hat{\phi}$ is the estimate of the dead-zone parameter $\phi$.

● ***Dynamic adaptation law for the slave:***

$$\dot{\hat{\boldsymbol{\theta}}}_s = -\Gamma_s \mathbf{Y}_s^T \mathbf{s}_\varepsilon \tag{21}$$

● ***Dead-zone adaptation law for the slave:***

$$\dot{\hat{\phi}} = -\eta \mathbf{E}_s^T \mathbf{s}_\varepsilon \tag{22}$$

where $\mathbf{\Gamma}_s \in \Re^{p\times p}$ is a diagonal positive-definite constant matrix and $\eta$ is a positive constant.

The control law for the slave (19) can be regarded as three composite parts. The first part, i.e., $m\mathbf{v}(t) + dz(\mathbf{v}(t))$, is the output of the dead-zone. The second part, i.e., $\boldsymbol{\tau}_e$,

is the local force feedback at the slave side which is fed to the slave controller, and the third part, i.e., $C_3(\boldsymbol{\tau}_h - \boldsymbol{\tau}_e)$, implements force tracking between the slave and the master. Besides, in the first part $\mathbf{v}(t)$ itself further includes four terms. The first term $-\mathbf{K}_s\mathbf{s}_s$ is a feedback law involving the velocity and position tracking errors between the slave and the master, the second term $\hat{\phi}\mathbf{E}_s$ compensates for the unknown dead-zone, the third term $\mathbf{Y}_s\hat{\boldsymbol{\theta}}_s$ compensates for the dynamic uncertainties. The forth term $\mathbf{K}_s^* sat(\frac{\mathbf{s}_s}{\varepsilon})$ is added to avoid using the sliding error vector $\mathbf{s}_s$ in the adaptive laws in case of chattering and compensate for the bounded function $|dz_i(v_i(t))| \le \alpha$, where $\alpha$ is the upper-bound. These four terms together perform adaptive position control for the slave ((as shown in the lower dashed box in Fig. 2). The estimate $\hat{\boldsymbol{\theta}}_s$ is updated by the dynamic adaptation law (21) and $\hat{\phi}$ is undated by the dead-zone adaptation law in (22).

Substituting (19)-(20) into (18), we can obtain the closed-loop equation for the slave:

$$\begin{aligned}&\mathbf{M}_s(\mathbf{q}_s)\dot{\mathbf{s}}_s - \mathbf{M}_s(\mathbf{q}_s)\boldsymbol{\Lambda}_s\Delta\dot{\mathbf{x}}_s(t) + \mathbf{M}_s(\mathbf{q}_s)\ddot{\mathbf{q}}_m + \mathbf{Y}_{s1}\boldsymbol{\theta}_{s*} + \mathbf{Y}_{s2}\boldsymbol{\theta}_{s*}\\ &= m[-\mathbf{K}_s\mathbf{s}_s + \hat{\phi}\mathbf{E}_s + \mathbf{Y}_s\hat{\boldsymbol{\theta}}_s - \mathbf{K}_s^* sat(\frac{\mathbf{s}_s}{\varepsilon})] + dz(\mathbf{v}(t)) + C_3(\boldsymbol{\tau}_h - \boldsymbol{\tau}_e)\end{aligned} \tag{23}$$

Using the definition of $\mathbf{E}_s$, (23) can be rewritten as:

$$\begin{aligned}&\mathbf{M}_s(\mathbf{q}_s)\dot{\mathbf{s}}_s\\ &= -\mathbf{M}_s(\mathbf{q}_s)\mathbf{E}_s - \mathbf{Y}_{s1}\boldsymbol{\theta}_{s*} - \mathbf{Y}_{s2}\boldsymbol{\theta}_{s*} + m[-\mathbf{K}_s\mathbf{s}_s + \hat{\phi}\mathbf{E}_s + \mathbf{Y}_s\hat{\boldsymbol{\theta}}_s - \mathbf{K}_s^* sat(\frac{\mathbf{s}_s}{\varepsilon})]\\ &+ dz(\mathbf{v}(t)) + C_3(\boldsymbol{\tau}_h - \boldsymbol{\tau}_e)\end{aligned} \tag{24}$$

Now, multiplying both sides of (13) by $C_3/C_2$ we have:

$$C_3/C_2\,[\mathbf{M}_m(\mathbf{q}_m)\dot{\mathbf{s}}_m + \mathbf{C}_m(\mathbf{q}_m, \dot{\mathbf{q}}_m)\mathbf{s}_m] = C_3/C_2\,(-\mathbf{K}_m\mathbf{s}_m + \mathbf{Y}_{mr}\Delta\boldsymbol{\theta}_m) + C_3(\boldsymbol{\tau}_h - \boldsymbol{\tau}_e) \tag{25}$$

Then, subtracting (25) from (24) gives a unified closed-loop equation for the entire master-slave system as:

$$\begin{aligned}
&\mathbf{M}_s(\mathbf{q}_s)\dot{\mathbf{s}}_s - C_3/C_2\,\mathbf{M}_m(\mathbf{q}_m)\dot{\mathbf{s}}_m \\
&= -\mathbf{M}_s(\mathbf{q}_s)\mathbf{E}_s - \mathbf{Y}_{s1}\boldsymbol{\theta}_{s*} - \mathbf{Y}_{s2}\boldsymbol{\theta}_{s*} \\
&+m[-\mathbf{K}_s\mathbf{s}_s + \hat{\phi}\mathbf{E}_s + \mathbf{Y}_s\hat{\boldsymbol{\theta}}_s - \mathbf{K}_s{}^{*}sat(\frac{\mathbf{s}_s}{\varepsilon})] + dz(\mathbf{v}(t)) \\
&-C_3/C_2\,(-\mathbf{K}_m\mathbf{s}_m + \mathbf{Y}_{mr}\Delta\boldsymbol{\theta}_m) + C_3/C_2\,\mathbf{C}_m(\mathbf{q}_m,\dot{\mathbf{q}}_m)\mathbf{s}_m
\end{aligned} \tag{26}$$

## 4. STABILITY AND TRANSPARENCY ANALYSIS

***Theorem 1:*** Assume the nonlinear teleoperation system (1)-(2) has dynamic uncertainties (6) in the master, and simultaneous dynamic uncertainties (7) and unknown dead-zone (3) in the slave. If it is controlled by the control law for the master (11) using the dynamic adaptation law (12) and by the control law for the slave (19)-(20) using the dynamic and dead-zone adaptation laws (21)-(22), then the following three results can be obtained:

( i ) The signals $\mathbf{s}_m$, $\mathbf{s}_\varepsilon$, $\Delta\boldsymbol{\theta}_m$, $\Delta\boldsymbol{\theta}_s$ and $\Delta\phi$ are all bounded.

( ii ) The position tracking error $\Delta\mathbf{q}_m = \mathbf{q}_m - \mathbf{q}_s$ converges to zero as $t \to \infty$.

(iii) The force tracking error $\Delta\boldsymbol{\tau} = \boldsymbol{\tau}_h - \boldsymbol{\tau}_e$ remains bounded. ■

***Proof:*** Consider the Lyapunov function candidate:

$$\begin{aligned}
V = &\frac{1}{2}C_3/C_2\,[\mathbf{s}_m{}^T\mathbf{M}_m(\mathbf{q}_m)\mathbf{s}_m + \Delta\boldsymbol{\theta}_m{}^T\boldsymbol{\Gamma}_m{}^{-1}\Delta\boldsymbol{\theta}_m)] \\
&+\frac{1}{2}[\frac{1}{m}\mathbf{s}_\varepsilon{}^T\mathbf{M}_s(\mathbf{q}_s)\mathbf{s}_\varepsilon + \Delta\boldsymbol{\theta}_s{}^T\boldsymbol{\Gamma}_s{}^{-1}\Delta\boldsymbol{\theta}_s + \frac{1}{\eta}\Delta\phi^2]
\end{aligned} \tag{27}$$

where $\Delta\boldsymbol{\theta}_s = \hat{\boldsymbol{\theta}}_s - \boldsymbol{\theta}_s$ and $\Delta\phi = \hat{\phi} - \phi$. Differentiating $V$ and using the fact that $\mathbf{s}_\varepsilon{}^T\mathbf{M}_s(\mathbf{q}_s)\dot{\mathbf{s}}_\varepsilon = \mathbf{s}_\varepsilon{}^T\mathbf{M}_s(\mathbf{q}_s)\dot{\mathbf{s}}_s$ gives us:

$$\begin{aligned}
\dot{V} = &C_3/C_2\,\mathbf{s}_m{}^T\mathbf{M}_m(\mathbf{q}_m)\dot{\mathbf{s}}_m + \frac{1}{2}C_3\Big/C_2\,\mathbf{s}_m{}^T\dot{\mathbf{M}}_m(\mathbf{q}_m)\mathbf{s}_m + C_3/C_2\,\Delta\boldsymbol{\theta}_m{}^T\boldsymbol{\Gamma}_m{}^{-1}\Delta\dot{\boldsymbol{\theta}}_m \\
&+\frac{1}{m}\mathbf{s}_\varepsilon{}^T\mathbf{M}_s(\mathbf{q}_s)\dot{\mathbf{s}}_s + \Delta\boldsymbol{\theta}_s{}^T\boldsymbol{\Gamma}_s{}^{-1}\dot{\hat{\boldsymbol{\theta}}}_s + \frac{1}{\eta}\Delta\phi\dot{\hat{\phi}} + \frac{1}{2m}\mathbf{s}_\varepsilon{}^T\dot{\mathbf{M}}_s\mathbf{s}_\varepsilon
\end{aligned} \tag{28}$$

From (26), we could get the expressions of $\mathbf{M}_m(\mathbf{q}_m)\dot{\mathbf{s}}_m$ and $\mathbf{M}_s(\mathbf{q}_s)\dot{\mathbf{s}}_s$, respectively. Then substituting the expressions of $\mathbf{M}_m(\mathbf{q}_m)\dot{\mathbf{s}}_m$ and $\mathbf{M}_s(\mathbf{q}_s)\dot{\mathbf{s}}_s$ into (28) and using Property 2 and the definitions of $\mathbf{Y}_s$, $\boldsymbol{\theta}_s$ and $\phi$ gives us:

$$\begin{aligned}\dot{V} = & C_3/C_2\,\Delta\boldsymbol{\theta}_m{}^T(\boldsymbol{\Gamma}_m{}^{-1}\Delta\dot{\boldsymbol{\theta}}_m + \mathbf{Y}_{mr}{}^T\mathbf{s}_m) - C_3/C_2\,\mathbf{s}_m{}^T\mathbf{K}_m\mathbf{s}_m \\ & -\mathbf{s}_\varepsilon{}^T\mathbf{K}_s\mathbf{s}_s + \mathbf{s}_\varepsilon{}^T[\hat{\phi}\mathbf{E}_s + \mathbf{Y}_s\hat{\boldsymbol{\theta}}_s - \mathbf{K}_s{}^* sat(\frac{\mathbf{s}_s}{\varepsilon})] \\ & +\mathbf{s}_\varepsilon{}^T(-\phi\mathbf{M}_s(\mathbf{q}_s)\mathbf{E}_s - \mathbf{Y}_s\boldsymbol{\theta}_s) + \mathbf{s}_\varepsilon{}^T\frac{dz(\mathbf{v}(t))}{m} \\ & +\Delta\boldsymbol{\theta}_s{}^T\boldsymbol{\Gamma}_s{}^{-1}\dot{\hat{\boldsymbol{\theta}}}_s + \frac{1}{\eta}\Delta\phi\dot{\hat{\phi}} + \frac{1}{2m}\mathbf{s}_\varepsilon{}^T\dot{\mathbf{M}}_s(\mathbf{q}_s)\mathbf{s}_\varepsilon\end{aligned} \tag{29}$$

Substituting the adaptive laws (12), (21) and (22) into (29), and using the definition of $\mathbf{W}_E$, we have:

$$\dot{V} = -C_3/C_2\,\mathbf{s}_m{}^T\mathbf{K}_m\mathbf{s}_m - \mathbf{s}_\varepsilon{}^T\mathbf{K}_s\mathbf{s}_s - \mathbf{s}_\varepsilon{}^T(t)\mathbf{K}_s{}^* sat(\frac{\mathbf{s}_s}{\varepsilon}) + \mathbf{s}_\varepsilon{}^T\frac{dz(\mathbf{v}(t))}{m} + \frac{1}{2m}\mathbf{s}_\varepsilon{}^T\dot{\mathbf{M}}_s(\mathbf{q}_s)\mathbf{s}_\varepsilon \tag{30}$$

Substituting (16) into (30) we can obtain:

$$\begin{aligned}\dot{V}(t) = & -C_3/C_2\,\mathbf{s}_m{}^T\mathbf{K}_m\mathbf{s}_m - \mathbf{s}_\varepsilon{}^T\mathbf{K}_s[\mathbf{s}_\varepsilon + \varepsilon sat(\frac{\mathbf{s}_s}{\varepsilon})] \\ & -\mathbf{s}_\varepsilon{}^T\mathbf{K}_s{}^* sat(\frac{\mathbf{s}_s}{\varepsilon}) + \mathbf{s}_\varepsilon{}^T\frac{dz(\mathbf{v}(t))}{m} + \frac{1}{2m}\mathbf{s}_\varepsilon{}^T\dot{\mathbf{M}}_s(\mathbf{q}_s)\mathbf{s}_\varepsilon \\ = & -C_3/C_2\,\mathbf{s}_m{}^T\mathbf{K}_m\mathbf{s}_m - \mathbf{s}_\varepsilon{}^T\mathbf{K}_s\mathbf{s}_\varepsilon - \mathbf{s}_\varepsilon{}^T(\mathbf{K}_s\varepsilon + \mathbf{K}_s{}^* )sat(\frac{\mathbf{s}_s}{\varepsilon}) \\ & +\mathbf{s}_\varepsilon{}^T\frac{dz(\mathbf{v}(t))}{m} + \frac{1}{2m}\mathbf{s}_\varepsilon{}^T\dot{\mathbf{M}}_s(\mathbf{q}_s)\mathbf{s}_\varepsilon \\ \le & -C_3/C_2\,\mathbf{s}_m{}^T\mathbf{K}_m\mathbf{s}_m - \mathbf{s}_\varepsilon{}^T\mathbf{K}_s\mathbf{s}_\varepsilon - eig_{\min}(\mathbf{K}_s\varepsilon + \mathbf{K}_s{}^* ).\|\mathbf{s}_\varepsilon\| \\ & +\mathbf{s}_\varepsilon{}^T\frac{dz(\mathbf{v}(t))}{m} + \frac{1}{2m}\mathbf{s}_\varepsilon{}^T\dot{\mathbf{M}}_s(\mathbf{q}_s)\mathbf{s}_\varepsilon \\ \le & -C_3/C_2\,\mathbf{s}_m{}^T\mathbf{K}_m\mathbf{s}_m - \mathbf{s}_\varepsilon{}^T\mathbf{K}_s\mathbf{s}_\varepsilon - [eig_{\min}(\mathbf{K}_s\varepsilon + \mathbf{K}_s{}^* ) \\ & -\frac{\|dz(\mathbf{v}(t))\|}{m} - \frac{\|\dot{\mathbf{M}}_s(\mathbf{q}_s)\mathbf{s}_\varepsilon\|}{2m}].\|\mathbf{s}_\varepsilon\| \\ \le & -C_3/C_2\,\mathbf{s}_m{}^T\mathbf{K}_m\mathbf{s}_m - \mathbf{s}_\varepsilon{}^T\mathbf{K}_s\mathbf{s}_\varepsilon - [eig_{\min}(\mathbf{K}_s\varepsilon + \mathbf{K}_s{}^* ) \\ & -\frac{\alpha}{m} - \frac{\beta}{2m}].\|\mathbf{s}_\varepsilon\|\end{aligned} \tag{31}$$

As aforementioned $eig_{\min}(\mathbf{K}_s\varepsilon + \mathbf{K}_s{}^* ) \ge \frac{\alpha}{m} + \frac{\beta}{2m}$, we have:

$$\dot{V} \le -C_3/C_2\, \mathbf{s}_m{}^T \mathbf{K}_m \mathbf{s}_m - \mathbf{s}_\varepsilon{}^T \mathbf{K}_s \mathbf{s}_\varepsilon \le 0 \tag{32}$$

From (27) and (32), we know that $V$ is positive-definite and $\dot{V}$ is negative semi-definite. Therefore, $V$ is bounded. Hence, the signals $\mathbf{s}_m$, $\Delta\boldsymbol{\theta}_m$, $\mathbf{s}_\varepsilon$, $\Delta\boldsymbol{\theta}_s$ and $\Delta\phi$ are bounded. This concludes the proof of ( i ) in Theorem 1.

In terms of position tracking, the definition $\mathbf{s}_m = \Delta\dot{\mathbf{q}}_m + \boldsymbol{\Lambda}_m \Delta\mathbf{q}_m$ represents a stable first-order system in $\Delta\mathbf{q}_m$ with $\mathbf{s}_m$ as an input, which has a pole at $-\boldsymbol{\Lambda}_m$ in the left-half of the complex plane as $\boldsymbol{\Lambda}_m$ is positive definite. Thus, the boundedness of $\mathbf{s}_m$ amounts to the boundedness of $\Delta\mathbf{q}_m$ and $\Delta\dot{\mathbf{q}}_m$, i.e., $\Delta\mathbf{q}_m, \Delta\dot{\mathbf{q}}_m \in L^\infty$. Moreover, from (32) we can obtain:

$$\begin{aligned} &C_3/C_2\, eig_{\min}(\mathbf{K}_m)\mathbf{s}_m^T\mathbf{s}_m + eig_{\min}(\mathbf{K}_s)\mathbf{s}_\varepsilon^T\mathbf{s}_\varepsilon \\ &\le C_3/C_2\, \mathbf{s}_m^T\mathbf{K}_m\mathbf{s}_m + \mathbf{s}_\varepsilon^T\mathbf{K}_s\mathbf{s}_\varepsilon \le -\dot{V} \end{aligned} \tag{33}$$

where $eig_{\min}(\mathbf{K}_m)$ and $eig_{\min}(\mathbf{K}_s)$ denote the minimum eigenvalues of the matrices $\mathbf{K}_m$ and $\mathbf{K}_s$, respectively. Integrating both sides of (33), we get:

$$\begin{aligned} &C_3/C_2\, eig_{\min}(\mathbf{K}_m)\int_0^t \|\mathbf{s}_m\|^2 dt + eig_{\min}(\mathbf{K}_s)\int_0^t \|\mathbf{s}_\varepsilon\|^2 dt \\ &\le -\int_0^t \dot{V} dt = V(0) - V(t) \le V(0) < \infty \end{aligned} \tag{34}$$

Hence, $\mathbf{s}_m, \mathbf{s}_\varepsilon \in L^2$, which is followed by $\Delta\mathbf{q}_m, \Delta\dot{\mathbf{q}}_m \in L^2$. Thus, according to Barbalat's Lemma [22], we have $\Delta\mathbf{q}_m = \mathbf{q}_m - \mathbf{q}_s \to 0$ as $t \to \infty$. This concludes the proof of ( ii ) in Theorem 1.

On the other hand, in terms of force tracking, we already have that $\mathbf{s}_m$, $\Delta\boldsymbol{\theta}_m$, $\mathbf{s}_\varepsilon$, $\Delta\boldsymbol{\theta}_s$ and $\Delta\phi$ are bounded. Since $\mathbf{s}_\varepsilon$ is bounded, we can readily get that $\mathbf{s}_s$ is bounded from (16). Then, according to (14), we can obtain that $\Delta\mathbf{x}_s$ is bounded. Moreover, it is possible to assume that $\ddot{\mathbf{q}}_m$ is bounded. Therefore, it can be seen that $\mathbf{E}_s$ is bounded from

its definition. Now, substituting (15) and the derivative of (8) into (26), (26) can be written as:

$$\begin{aligned}&\mathbf{M}_s(\mathbf{q}_s)(\boldsymbol{\Lambda}_s\Delta\mathbf{x}_s-\Delta\ddot{\mathbf{q}}_m)-C_3/C_2\,\mathbf{M}_m(\mathbf{q}_m)(\Delta\ddot{\mathbf{q}}_m+\boldsymbol{\Lambda}_m\Delta\dot{\mathbf{q}}_m)\\&=-\mathbf{M}_s(\mathbf{q}_s)\mathbf{E}_s-\mathbf{Y}_{s1}\boldsymbol{\theta}_{s*}-\mathbf{Y}_{s2}\boldsymbol{\theta}_{s*}\\&+m[-\mathbf{K}_s\mathbf{s}_s+\hat{\phi}\mathbf{E}_s+\mathbf{Y}_s\hat{\boldsymbol{\theta}}_s-\mathbf{K}_s^{*}sat(\frac{\mathbf{s}_s}{\varepsilon})]+dz(\mathbf{v}(t))\\&-C_3/C_2\,(-\mathbf{K}_m\mathbf{s}_m+\mathbf{Y}_{mr}\Delta\boldsymbol{\theta}_m)+C_3/C_2\,\mathbf{C}_m(\mathbf{q}_m,\dot{\mathbf{q}}_m)\mathbf{s}_m\end{aligned}\tag{35}$$

Because $\Delta\boldsymbol{\theta}_m$, $\Delta\boldsymbol{\theta}_s$ and $\Delta\phi$ are bounded, we can readily have $\hat{\boldsymbol{\theta}}_m$, $\hat{\boldsymbol{\theta}}_s$ and $\hat{\phi}$ are bounded. In addition, $\boldsymbol{\theta}_{s*}$ is dynamic parameter vector which is a constant. Also, $dz(\mathbf{v}(t))$ is bounded as aforementioned in (5). Then it can be seen from (35) that $\Delta\ddot{\mathbf{q}}_m$ is bounded, which results in the boundedness of $\dot{\mathbf{s}}_m$ and $\dot{\mathbf{s}}_s$ according to (8) and (15), respectively. Then according to (23) we can finally get that $\Delta\boldsymbol{\tau}=\boldsymbol{\tau}_h-\boldsymbol{\tau}_e$ is bounded as $t\to\infty$. This concludes the proof of (iii) in Theorem 1. ■

## 5 SIMULATIONS

The simulations are performed with two 2-DOF planar rehabilitation robots where dead-zone is added to the slave robot joints in order to accord with the situation in this paper. The dynamics of the rehabilitation robots are as follows [23]:

$$\mathbf{M}(\mathbf{q})=\begin{bmatrix}\alpha_1 & -\frac{1}{2}\alpha_2\sin(q_1-q_2)\\ -\frac{1}{2}\alpha_2\sin(q_1-q_2) & \alpha_3\end{bmatrix},$$

$$\mathbf{C}(\mathbf{q},\dot{\mathbf{q}})=\begin{bmatrix}0 & \frac{1}{2}\alpha_2\sin(q_1-q_2)\dot{q}_2\\ \frac{1}{2}\alpha_2\sin(q_1-q_2)\dot{q}_1 & 0\end{bmatrix},$$

where $\alpha_1$=0.06256 , $\alpha_2$=0.00289 and $\alpha_3$=0.04194 are constants, and $q_1$ and $q_2$ are the positions of joint 1 and joint 2. Due to the planar configurations, gravity terms are ignored. Moreover, the dead-zone added to the slave robot joints is taken as: $m$=1 , $b_l$=-15 and $b_r$=15 .

Then according to Property.1, the dynamic parameter vector of the master and the slave can be found as $\boldsymbol{\theta}_m = \boldsymbol{\theta}_{s^*} = [\alpha_1, \alpha_2, \alpha_3]^T$ . More details about the calculation of $\boldsymbol{\theta}_m$ , $\mathbf{Y}_m$ , $\mathbf{Y}_{mr}$ , $\boldsymbol{\theta}_{s^*}$ , $\boldsymbol{\theta}_s$ and $\mathbf{Y}_s$ can be found in the Appendix.

In the simulations, the dynamic parameters have inaccurate initial values, i.e., $\hat{\boldsymbol{\theta}}_m(0) = \hat{\boldsymbol{\theta}}_{s^*}(0) = [\hat{\alpha}_1(0), \hat{\alpha}_2(0), \hat{\alpha}_3(0)]^T = [0.03128, 0.001445, 0.02097]^T$ , and the initial guess of the dead-zone parameter is $\hat{m}(0) = 0.5$ . Besides, the initial positions of the master and the slave are set randomly as $\mathbf{q}_m(0) = [0.5, 1.5]^T, \mathbf{q}_s(0) = [1, 1]^T$ .

The operator and the environment are considered to be second-order LTI models [6, 7]. The mass, damping, and stiffness parameters of the operator's hand (i.e., $m_h, b_h, k_h$) and the environment (i.e., $m_e, b_e, k_e$) are shown in Table 1.

Besides, for a realistic simulation, let $\boldsymbol{\tau}_h^*$ rise from a non-zero value, $\boldsymbol{\tau}_h^* = [\sin(0.1t), \sin(0.1t)]^T$. Also, take $\boldsymbol{\tau}_e^* = [0, 0]^T$ .

The parameters of the controllers for the master and the slave are shown in Table.2 where $\mathbf{I}$ is the identity matrix with proper dimension. In addition, we set $\boldsymbol{\Lambda}_{ts} = \begin{bmatrix} 1 & 1 & 1 & 0 \\ 1 & 1 & 0 & 1 \end{bmatrix}$ and $\boldsymbol{\Lambda}_s = \begin{bmatrix} 0 & 0 & 1 & 1 \\ 0 & 0 & 1 & 1 \end{bmatrix}$ . The simulations results in contact motion are shown in Fig.3-Fig.6.

Fig.3 and Fig.4 illustrate the comparison of the position tracking performance. In Fig.3, when the conventional adaptive control which merely deals with dynamic uncertainties is employed, there exists obvious position tracking error both in joint 1 and joint 2, especially when the zero position is crossed. In comparison, in Fig.4, when the proposed adaptive control which deals with both dynamic uncertainties and dead-zone is applied, as expected, the slave can well track the position of the master well both in joint 1 and joint 2. The tracking performance is satisfying even when the zero position is crossed.

Fig.5 and Fig.6 show the force tracking performance. As it can be seen in Fig.5 the force tracking neither in joint 1 nor in joint 2 is far from ideal case—the force tracking error is quite undesirable at the time about 3s, 6s, 9s, 12s, 15s, 18s when the zero force is crossed. On the contrary, the slave can track the force of the master in a satisfying way in Fig.6 where the proposed adaptive control which deals with both dynamic uncertainties and dead-zone is applied. The reason for the results above is that the conventional adaptive control cannot compensate for the unknown dead-zone in $\phi$, while the proposed adaptive control can compensate for both the dynamic uncertainties in $\boldsymbol{\theta}_m$ and $\boldsymbol{\theta}_s$, and the unknown dead-zone in $\phi$.

***Remark 1:*** It is worth noting that in adaptive control, the tracking error should converge regardless of whether the input is persistently exciting or not, i.e., model parameter convergence should not be a prerequisite for tracking error convergence. As can be seen from the proof of Theorem 1, position tracking error converges to zero as $t \to \infty$, and the force tracking error can remain bounded regardless of the convergence of model parameters $\boldsymbol{\theta}_m$, $\boldsymbol{\theta}_s$ and $\phi$.

In the adaptive control law (11) and (19) $\boldsymbol{\tau}_h$ and $\boldsymbol{\tau}_e$ are communicated from the master and the slave to each other and can be measured by sensors. From the unified closed-loop equation (26) and the proof of Therom 1 it can be seen that using the proposed adaptive controller position and force tracking can be obtained without requiring any dynamic model of the human operator or the environment. This is especially beneficial since in real teleoperation systems where the dynamic parameters of the human operator and the environment are uncertain and it is difficult to their exact dynamic models. However, as we know it is unavoidable that there is noise in sensor measurement. Thus, in order to see how the proposed controller will work under noise in sensor measurement, we introduce Gaussian distributed noise in the force measurements in the simulation. The corresponding results are shown in Fig. 7-Fig.10.

Fig.7 and Fig.8 illustrate the position tracking with measurement noise. Comparing Fig.7 with Fig.8, we can see that with the conventional adaptive control the position tracking error is obviously much bigger especially at the time about 3s, 5s, 9s, 16s and 18s due to noise in the signals, while the position trajectories of the master and the slave are very close to one another.

Fig.9 and Fig.10 compare the force tracking performance of the conventional adaptive control and the proposed adaptive control. The measurement noise greatly decreased the force tracking performance in Fig.9, while it does not have obvious influence in Fig.10.

Furthermore, in order to analyze the position and force tracking errors with measurement noise quantitatively, the mathematical index MSE (Mean Square Error) is

utilized and the calculation result is shown in Table 3, where the MSE is calculated with the following equations:

$$MSE_{q_1} = \sqrt{\frac{1}{N}(\sum_{j=1}^{N} q_{m_1} - q_{s_1})}\,,\ MSE_{q_2} = \sqrt{\frac{1}{N}(\sum_{j=1}^{N} q_{m_2} - q_{s_2})} \tag{36}$$

$$MSE_{\tau_1} = \sqrt{\frac{1}{N}(\sum_{j=1}^{N} \tau_{h_1} - \tau_{e_1})}\,,\ MSE_{\tau_2} = \sqrt{\frac{1}{N}(\sum_{j=1}^{N} \tau_{h_2} - \tau_{e_2})} \tag{37}$$

where $MSE_q$ and $MSE_\tau$ are the MSEs of the position and force tracking, respectively. N is the sampling number. The subscripts *1* and *2* denote the first and the second joints, respectively.

As shown in Table 3, when there is measurement noise the position tracking error of the conventional adaptive control is obviously bigger and the force tracking performance significantly losses. Compared to the conventional scheme, both the position and force tracking errors are greatly improved even with measurement noise when the proposed scheme is employed.

## 6. CONCLUSIONS

This paper addresses the design of an adaptive control for intrinsically nonlinear teleoperation systems to simultaneously deal with dynamic uncertainties and unknown dead-zone. Two adaptive controllers are designed for the master and the slave, respectively, and then incorporated into the 4-channel teleoperation architecture. The proposed scheme has improved the position and force tracking performance compared to the conventional adaptive scheme when the dead-zone and the dynamics of the robots are

uncertain. The extension of the presented techniques to deal with communication delay [24] remains as future work.

## ACKNOWLEDGEMENTS

This research was supported by Sichuan Youth Science &Technology Foundation under Grant 2017JQ0022, the Key Scientific Research Project of Sichuan Provincial Department of Education under Grant 17ZA0359, the National Natural Science Foundation of China under Grant 61305104, the Scientific and Technical Supporting Programs of Sichuan Province under Grant 2016GZ0395, and the Natural Sciences and Engineering Research Council of Canada.

## APPENDIX: CALCULATION OF $\boldsymbol{\theta}_m$, $\mathbf{Y}_m$, $\mathbf{Y}_{mr}$, $\boldsymbol{\theta}_{s^*}$, $\boldsymbol{\theta}_s$ AND $\mathbf{Y}_s$

The dynamics of the rehabilitation robots are as follows [17]:

$$\mathbf{M}(\mathbf{q})\ddot{\mathbf{q}} + \mathbf{C}(\mathbf{q},\dot{\mathbf{q}})\dot{\mathbf{q}} = \boldsymbol{\tau}$$

where $\mathbf{M}(\mathbf{q})$ and $\mathbf{C}(\mathbf{q},\dot{\mathbf{q}})$ take the following forms:

$$\mathbf{M}(\mathbf{q}) = \begin{bmatrix} \alpha_1 & -\frac{1}{2}\alpha_2 \sin(q_1 - q_2) \\ -\frac{1}{2}\alpha_2 \sin(q_1 - q_2) & \alpha_3 \end{bmatrix},$$

$$\mathbf{C}(\mathbf{q},\dot{\mathbf{q}}) = \begin{bmatrix} 0 & \frac{1}{2}\alpha_2 \sin(q_1 - q_2)\dot{q}_2 \\ \frac{1}{2}\alpha_2 \sin(q_1 - q_2)\dot{q}_1 & 0 \end{bmatrix}.$$

Then we can get:

$$\mathbf{M}(\mathbf{q})\ddot{\mathbf{q}}+\mathbf{C}(\mathbf{q},\dot{\mathbf{q}})\dot{\mathbf{q}}=\begin{bmatrix}\alpha_1\ddot{q}_1-\frac{1}{2}\alpha_2\sin(q_1-q_2)(\ddot{q}_2-\dot{q}_2{}^2)\\ \alpha_3\ddot{q}_2-\frac{1}{2}\alpha_2\sin(q_1-q_2)(\ddot{q}_1-\dot{q}_1{}^2)\end{bmatrix}.$$

Applying Property 1, we can obtain：

$$\boldsymbol{\theta}_m=\begin{bmatrix}\alpha_1\\ \alpha_2\\ \alpha_3\end{bmatrix},$$

$$\mathbf{Y}_m=\begin{bmatrix}\ddot{q}_1 & -\frac{1}{2}\sin(q_1-q_2)(\ddot{q}_2-\dot{q}_2{}^2) & 0\\ 0 & -\frac{1}{2}\sin(q_1-q_2)(\ddot{q}_1-\dot{q}_1{}^2) & \ddot{q}_2\end{bmatrix}.$$

Since we have got $\boldsymbol{\theta}_m$ and the following equation from (10):

$$\mathbf{Y}_{mr}(\mathbf{q}_m,\dot{\mathbf{q}}_m,\dot{\mathbf{q}}_{mr},\ddot{\mathbf{q}}_{mr})\boldsymbol{\theta}_m=\mathbf{M}_m(\mathbf{q}_m)\ddot{\mathbf{q}}_{mr}+\mathbf{C}_m(\mathbf{q}_m,\dot{\mathbf{q}}_m)\dot{\mathbf{q}}_{mr}+\mathbf{G}_m(\mathbf{q}_m),$$

we can obtain that :

$$\mathbf{Y}_{mr}=\begin{bmatrix}\ddot{q}_{mr_1} & \frac{1}{2}\sin(q_1-q_2)(\dot{q}_2\dot{q}_{mr_2}-\ddot{q}_{mr_2}) & 0\\ 0 & \frac{1}{2}\sin(q_1-q_2)(\dot{q}_1\dot{q}_{mr_1}-\ddot{q}_{mr_1}) & \ddot{q}_{mr_2}\end{bmatrix}$$

where $q_{mr_1}$ and $q_{mr_2}$ are the two elements of $\mathbf{q}_{mr}=[q_{mr_1},q_{mr_2}]^T$.

As we can calculate that $\mathbf{C}(\mathbf{q},\dot{\mathbf{q}})\dot{\mathbf{q}}=\begin{bmatrix}\frac{1}{2}\alpha_2\sin(q_1-q_2)\dot{q}_2{}^2\\ \frac{1}{2}\alpha_2\sin(q_1-q_2)\dot{q}_1{}^2\end{bmatrix}$, then applying Property 1'

we can also obtain:

$$\boldsymbol{\theta}_{s*}=\begin{bmatrix}\alpha_1\\ \alpha_2\\ \alpha_3\end{bmatrix},$$

$$\mathbf{Y}_{s1}=\begin{bmatrix} 0 & \frac{1}{2}\sin(q_1-q_2)\dot{q}_2{}^2 & 0 \\ 0 & \frac{1}{2}\sin(q_1-q_2)\dot{q}_1{}^2 & 0 \end{bmatrix}.$$

Therefore, according to the definitions $\mathbf{Y}_s=\mathbf{Y}_{s1}+\mathbf{Y}_{s2}$ and $\boldsymbol{\theta}_s=\frac{1}{m}\boldsymbol{\theta}_{s*}$, we can finally get:

$$\boldsymbol{\theta}_{\mathrm{s}}=\frac{1}{m}\boldsymbol{\theta}_{\mathrm{s}*}=\frac{1}{m}\begin{bmatrix}\alpha_1\\ \alpha_2\\ \alpha_3\end{bmatrix},$$

$$\mathbf{Y}_{\mathrm{s}}=\mathbf{Y}_{s1}=\begin{bmatrix} 0 & \frac{1}{2}\sin(q_1-q_2)\dot{q}_2{}^2 & 0 \\ 0 & \frac{1}{2}\sin(q_1-q_2)\dot{q}_1{}^2 & 0 \end{bmatrix}.$$

## REFERENCES

[1] P. Hokayem, and M. Spong, "Bilateral teleoperation: An historical survey," Automatica, 2006, 42 (12): 2035-2057.

[2] W. Zhu, and S. E. Salcudean, "Stability guaranteed teleoperation: An adaptive motion/force control approach," IEEE transactions on automatic control, 2000, 45 (11): 1951-1969.

[3] N. V. Q. Hung, T. Narikiyo, and H. D. Tuan, "Nonlinear adaptive control of master-slave system in teleoperation," Control Engineering Practice, 2003, 11 (1): 1-10.

[4] N. Chopra, M. W. Spong, and R. Lozano, "Synchronization of bilateral teleoperators with time delay," Automatica, 2008, 44 (8): 2142-2148.

[5] E. Nuño, R. Ortega, and L. Basañez, "An adaptive controller for nonlinear teleoperators," Automatica, 2010, 46 (1): 155-159.

[6] F. Hashemzadeh, I. Hassanzadeh, and M. Tavakoli, "Teleoperation in the presence of varying time Delays and sandwich linearity in actuators," Automatica, 2013, 49 (9): pp. 2813–2821.

[7] X. Liu, R. Tao, and M. Tavakoli, "Adaptive Control of Uncertain Nonlinear Teleoperation Systems", Mechatronics, 2014, 24(1): 66-78.

[8] S. Islam, P. X. Liu, and A. EI Saddik, "Nonlinear adaptive control for teleoperation systems with symmetrical and unsymmetrical time-varying delay," International Journal of Systems Science, 2015, 46(16): 2928-2938.

[9] DH. Zhai, and YQ. Xia, "Adaptive control for teleoperation system with varying time delays and input saturation constraints," IEEE Transactions on Industrial Electronics, 2016, 63(11): 6921-6929.

[10] E. Franco, "Combined adaptive and predictive control for a teleoperation system with force disturbance and input delay," Frontiers in Robotics and AI, 2016, 3: 1-11.

[11] HQ. Wang, PX. Liu, and SC.Liu, "Adaptive neural synchronization control for bilateral teleoperation systems with time delay and backlash-like hysteresis," IEEE Transactions on Cybernetics, 2017, 47(10): 3018-3026.

[12] T. Abut, S. Soyguder, "Real-time control of bilateral teleoperation system with adaptive computed torque method," Industrial Robot-An International Journal, 2017, 44(3):299-311

[13] YL. Li, YX. Yin, DZ. Zhang, "Adaptive task-space synchronization control of bilateral teleoperation systems with uncertain parameters and communication delays", IEEE ACCESS, 2018, 6: 5740-5748.

[14] ZY. Lu, PF. Huang, and ZX. Liu, "Predictive approach for sensorless bimanual teleoperation under random time delays with adaptive fuzzy control", IEEE Transactions on Industrial Electronics, 2018, 65(3): 2439-2448.

[15] G. Tao, and P. V. Kokotovic, "Adaptive control of systems with actuator and sensor nonlinearities," New York: Wiley, 1996.

[16] M. L. Crradini, G. Orlando, and G. Parlangeli, "A VSC approach for the robust stabilization of nonlinear plants with uncertain nonsmooth actuator nonlinearities-a unified framework," IEEE Transactions on Automatic Control, 2004, 49 (5): 807-812.

[17] X. Wang, C. Su, and H. Hong, "Robust adaptive control of a class of nonlinear systems with unknown dead-zone", Automatica, 2004, 40 (3): 407-413.

[18] R. Kelly, V. Santibanez, and A. Loria, "Control of robot manipulators in joint space," Springer, Berlin, Germany, 2005.

[19] F. L. Lewis, W. K. Tim, L. Wang, and Z. Li, "Dead-zone compensation in motion control systems using adaptive fuzzy logic control," IEEE Transactions on Control Systems Technology, 1999, 7 (6): 731-741.

[20] M. Tavakoli, A. Aziminejad, R.V. Patel, et al, "High-fidelity bilateral teleoperation systems and the effect of multimodal haptics," IEEE Transactions on Systems, Man, and Cybernetics - Part B, 2007, 37 (6): 1512-1528.

[21] D. A. Lawrence, "Stability and transparency in bilateral teleoperation," IEEE Transactions on Robotics and Automation, 1993, 9 (5): 624-637.

[22] J. J. E. Slotine, and W. Li, "Applied nonlinear control", Prentice-Hall, Englewood Cliffs, NJ, 1991.

[23] M. Dyck, and M. Tavakoli, "Measuring the dynamic impedance of the human arm

without a force sensor," IEEE International Conference on Rehabilitation Robotics, Seattle, Washington USA, 2013: 978-985.

[24] L. Chan, F. Naghdy, and D. Stirling, "Application of adaptive controllers in teleopertion systems: a survey," IEEE Transactions on Human-manchine Systems, 2014, 44 (3): 337-352.

## Figure Caption List

Fig. 1 Dead-zone at the input of the slave robot

Fig. 2 Architecture of the proposed 4-channel adaptive teleoperation control

Fig.3 Positions and position errors for the conventional adaptive control. (a) Position of joint 1. (b) Position of joint 2. (c) Position error of joint 1. (d) Position error of joint 2.

Fig.4 Positions and position errors for the proposed adaptive control. (a) Position of joint 1. (b) Position of joint 2. (c) Position error of joint 1. (d) Position error of joint 2.

Fig. 5 Torques and torque errors for the conventional adaptive control. (a) Torque of joint 1. (b) Torque of joint 2. (c) Torque error of joint 1. (d) Torque error of joint 2.

Fig. 6 Torques and torque errors for the proposed adaptive control. (a) Torque of joint 1. (b) Torque of joint 2. (c) Torque error of joint 1. (d) Torque error of joint 2.

Fig.7 Positions for the conventional adaptive control with measurement noise. (a) Position of joint 1. (b) Position of joint 2.

Fig.8 Positions for the proposed adaptive control with measurement noise. (a) Position of joint 1. (b) Position of joint 2.

Fig.9 Torques for the conventional adaptive control with measurement noise. (a) Torque of joint 1. (b) Torque of joint 2.

Fig.10 Torques for the proposed adaptive control with measurement noise. (a) Torque of joint 1. (b) Torque of joint 2.

## Table Caption List

Table 1. Parameters of the operator and the environment

Table 2. Parameters of the controllers

Table3. Quantitative comparison of position and force tracking (with measurement noise)

Table 1. Parameters of the operator and the environment

| $m_h$ | $b_h$ | $k_h$ | $m_e$ | $b_e$ | $k_e$ |
|---|---|---|---|---|---|
| 0.2(kg) | 50(Nsm$^{-1}$) | 1000(Nm$^{-1}$) | 0.1(kg) | 20(Nsm$^{-1}$) | 1000(Nm$^{-1}$) |

Table 2. Parameters of the controllers

| $\mathbf{K}_m$ | $\mathbf{\Gamma}_m$ | $\mathbf{\Lambda}_m$ | $C_2$ | $\mathbf{K}_s$ | $\mathbf{K}_s^*$ | $\mathbf{\Gamma}_s$ | $C_3$ | $\eta$ | $\varepsilon$ |
|---|---|---|---|---|---|---|---|---|---|
| $0.01\mathbf{I}$ | $0.1\mathbf{I}$ | $\mathbf{I}$ | 1 | $10\mathbf{I}$ | $10\mathbf{I}$ | $10\mathbf{I}$ | 1 | 5 | 0.1 |

Table3. Quantitative comparison of position and force tracking (with measurement noise)

| Method / Index(MSE) | Conventional adaptive control | Proposed adaptive control |
|---|---|---|
| $MSE_{q_1}$ | 0.2373 | 0.1286 |
| $MSE_{q_2}$ | 0.2779 | 0.2016 |
| $MSE_{\tau_1}$ | 0.4963 | 0.2135 |
| $MSE_{\tau_2}$ | 0.6713 | 0.2355 |

Journal of Dynamic Systems, Measurement and Control. Received February 18, 2016;
Accepted manuscript posted June 28, 2018. doi:10.1115/1.4040666


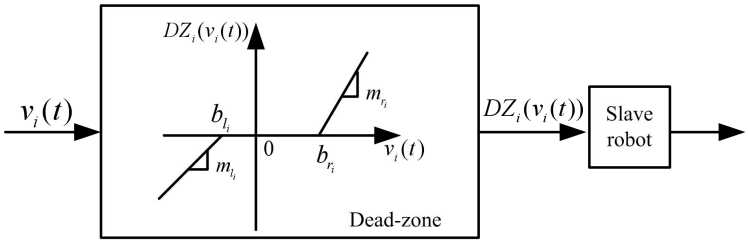


Fig. 1 Dead-zone at the input of the slave robot

Journal of Dynamic Systems, Measurement and Control. Received February 18, 2016;
Accepted manuscript posted June 28, 2018. doi:10.1115/1.4040666


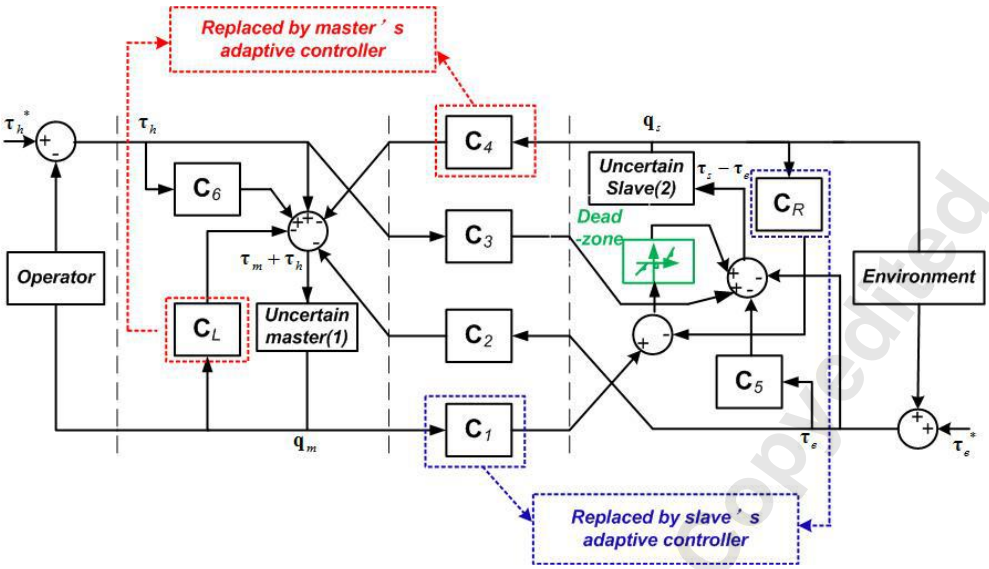


Fig. 2 Architecture of the proposed 4-channel adaptive teleoperation control

Journal of Dynamic Systems, Measurement and Control. Received February 18, 2016;
Accepted manuscript posted June 28, 2018. doi:10.1115/1.4040666


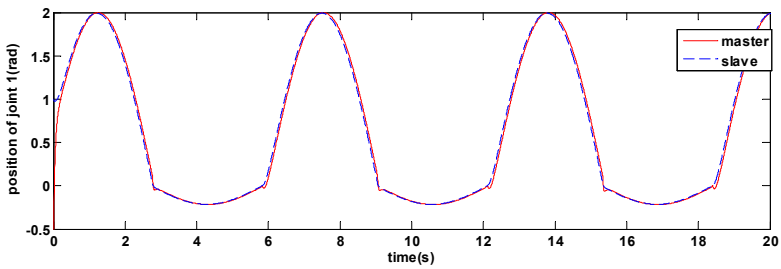


(a)

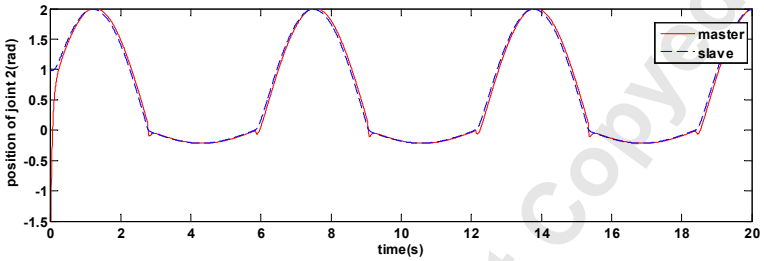


(b)

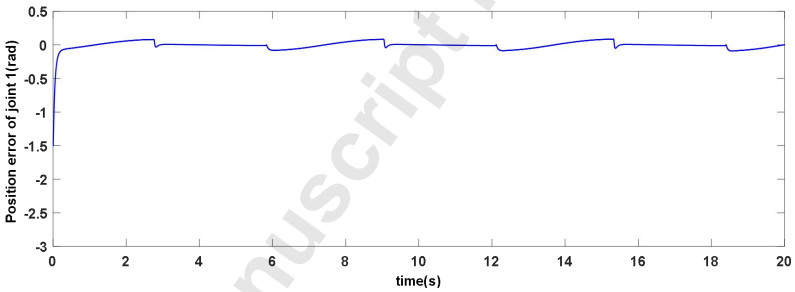


(c)

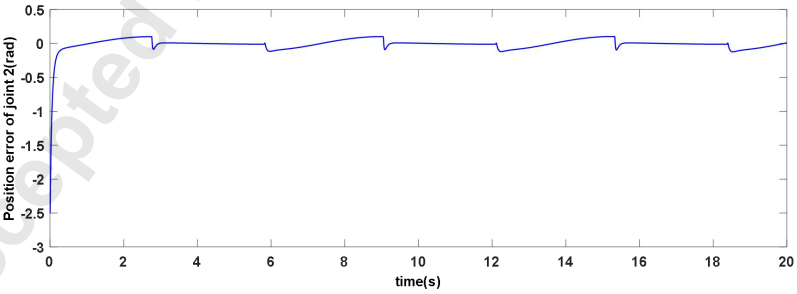


(d)

Fig.3 Positions and position errors for the conventional adaptive control. (a) Position of joint 1. (b) Position of joint 2. (c) Position error of joint 1. (d) Position error of joint 2.

Journal of Dynamic Systems, Measurement and Control. Received February 18, 2016;
Accepted manuscript posted June 28, 2018. doi:10.1115/1.4040666


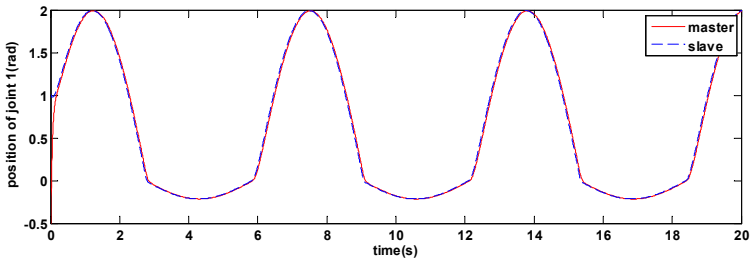


(a)

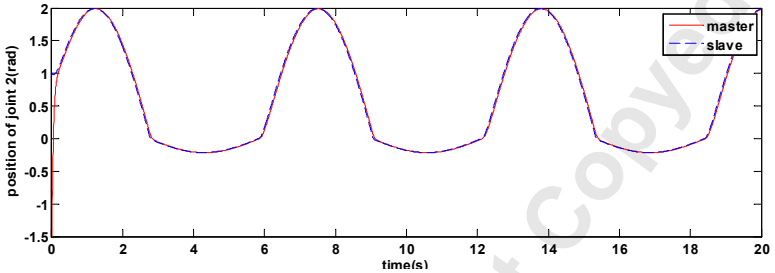


(b)

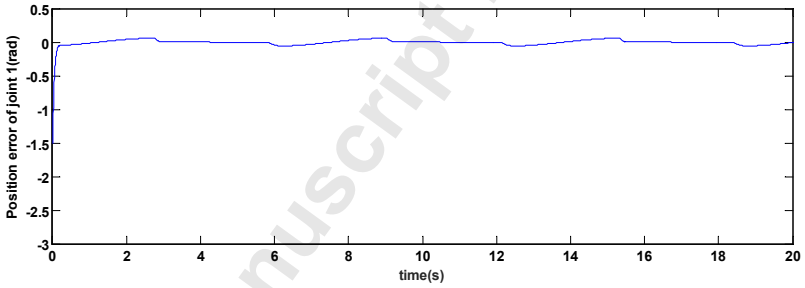


(c)

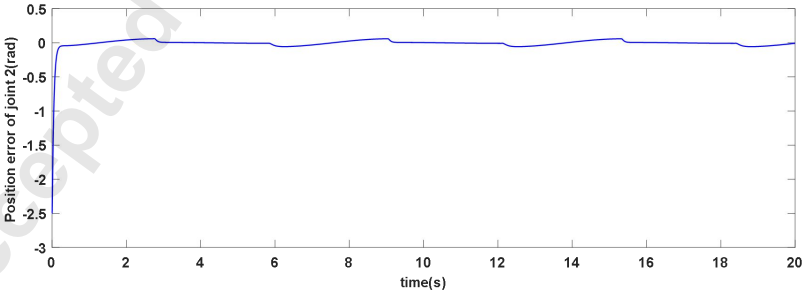


(d)

Fig.4 Positions and position errors for the proposed adaptive control. (a) Position of joint 1. (b) Position of joint 2. (c) Position error of joint 1. (d) Position error of joint 2.

Journal of Dynamic Systems, Measurement and Control. Received February 18, 2016;
Accepted manuscript posted June 28, 2018. doi:10.1115/1.4040666


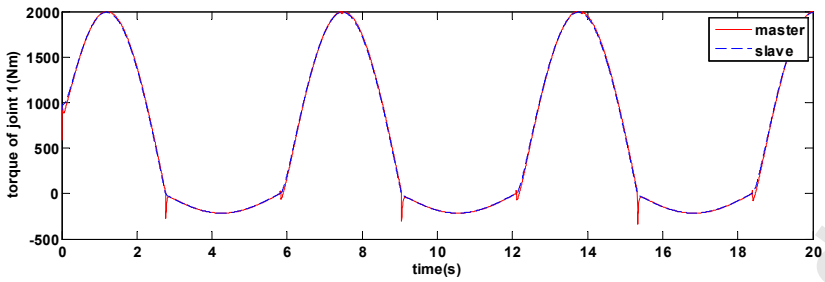


(a)

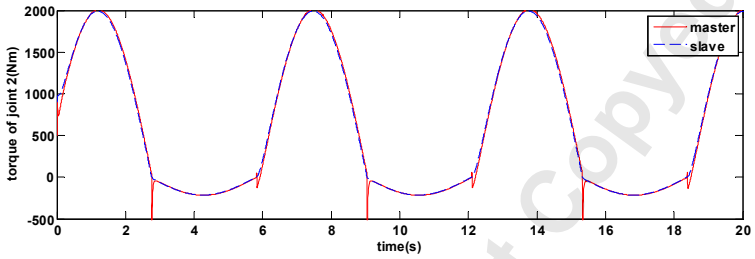


(b)

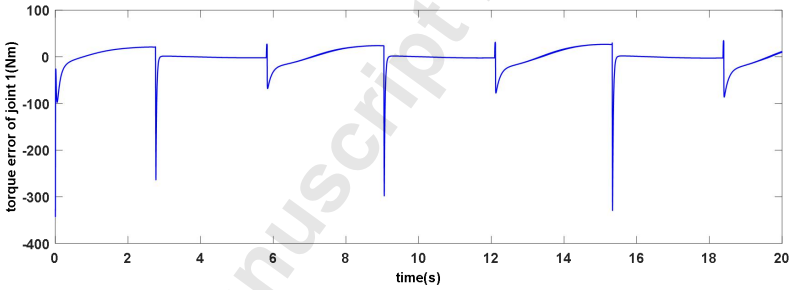


(c)

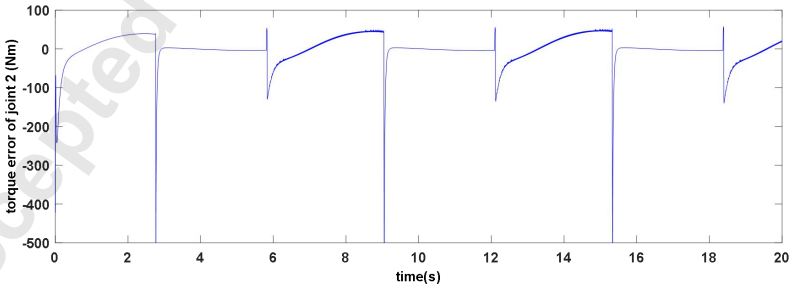


(d)

Fig. 5 Torques and torque errors for the conventional adaptive control. (a) Torque of joint 1. (b) Torque of joint 2. (c) Torque error of joint 1. (d) Torque error of joint 2.

Journal of Dynamic Systems, Measurement and Control. Received February 18, 2016;
Accepted manuscript posted June 28, 2018. doi:10.1115/1.4040666


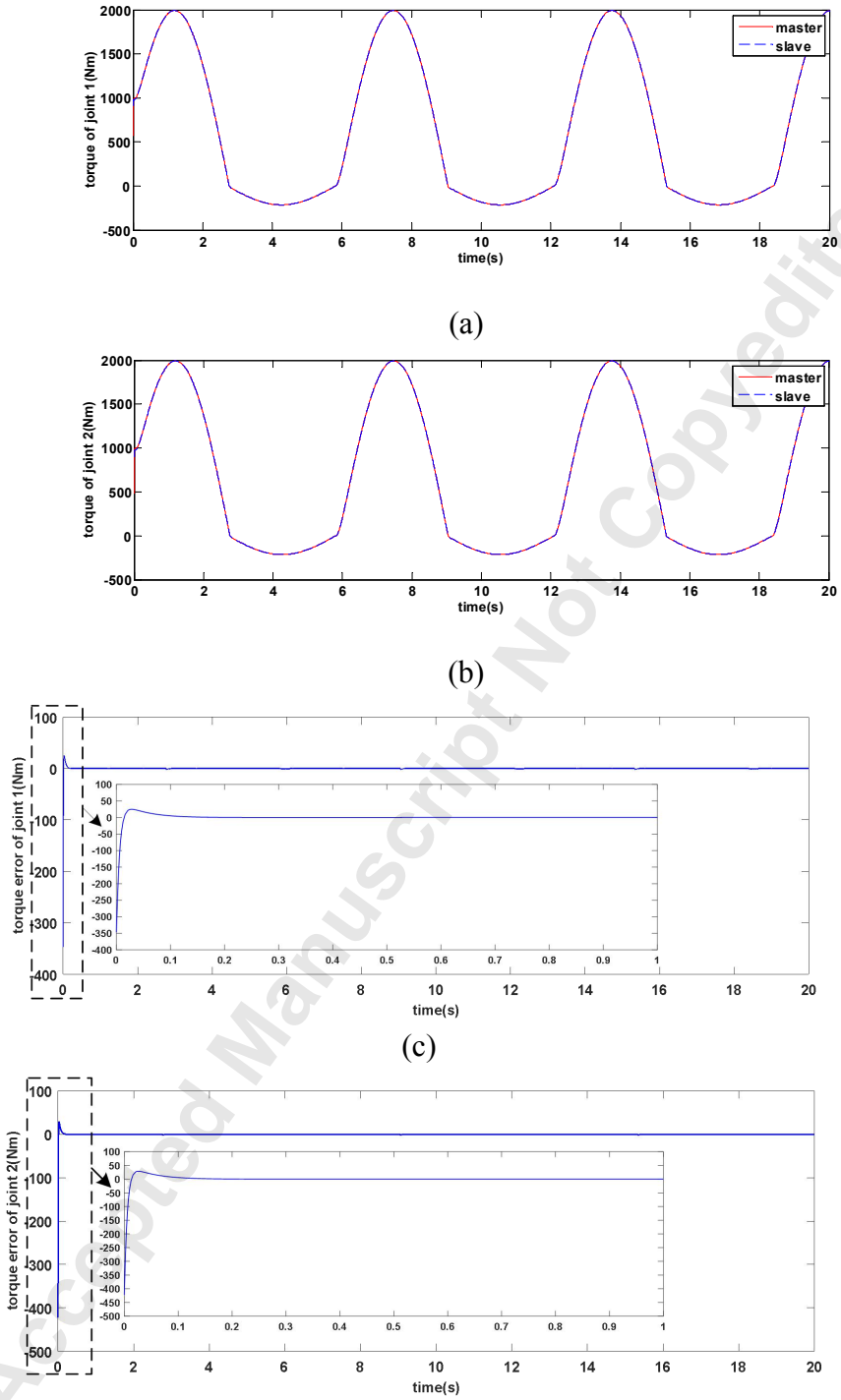


Fig. 6 Torques and torque errors for the proposed adaptive control. (a) Torque of joint 1. (b) Torque of joint 2. (c) Torque error of joint 1. (d) Torque error of joint 2.

Journal of Dynamic Systems, Measurement and Control. Received February 18, 2016;
Accepted manuscript posted June 28, 2018. doi:10.1115/1.4040666


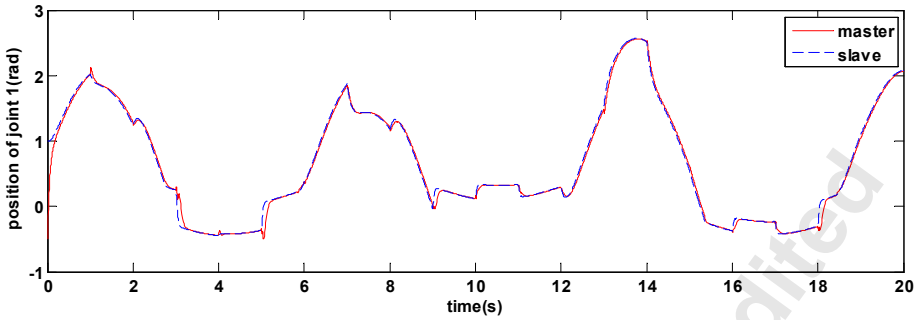


(a)

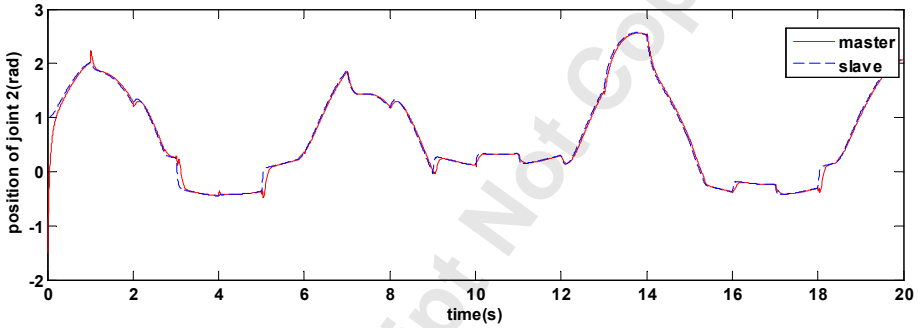


(b)

Fig.7 Positions for the conventional adaptive control with measurement noise. (a) Position of joint 1. (b) Position of joint 2.

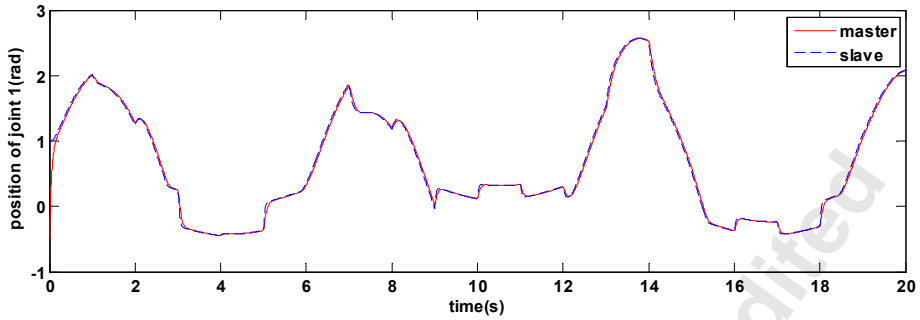


(a)

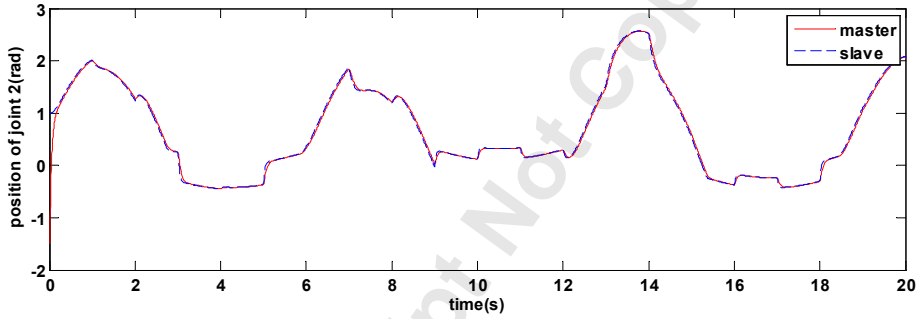


(b)

Fig.8 Positions for the proposed adaptive control with measurement noise. (a) Position of joint 1. (b) Position of joint 2.

Journal of Dynamic Systems, Measurement and Control. Received February 18, 2016;
Accepted manuscript posted June 28, 2018. doi:10.1115/1.4040666


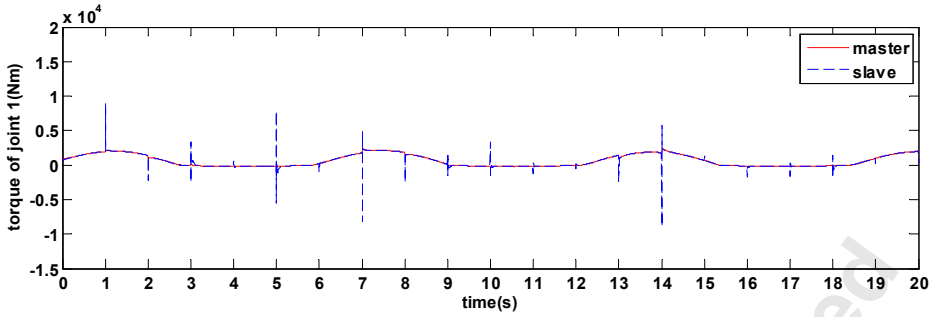


(a)

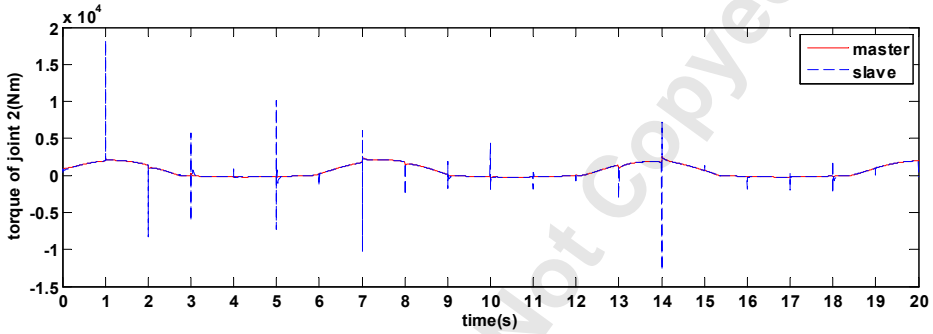


(b)

Fig.9 Torques for the conventional adaptive control with measurement noise. (a) Torque of joint 1. (b) Torque of joint 2.

Journal of Dynamic Systems, Measurement and Control. Received February 18, 2016;
Accepted manuscript posted June 28, 2018. doi:10.1115/1.4040666


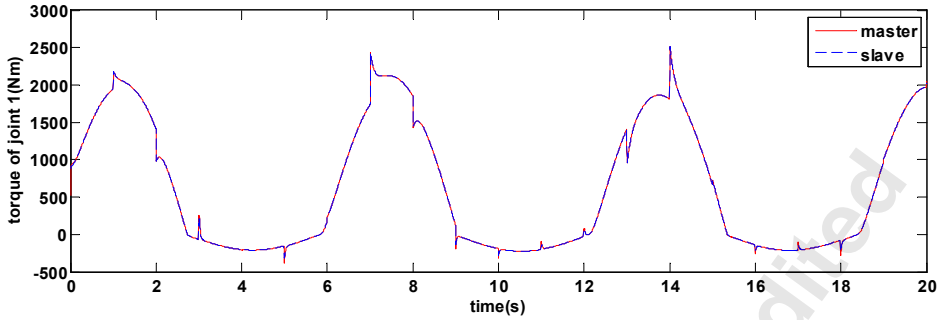


(a)

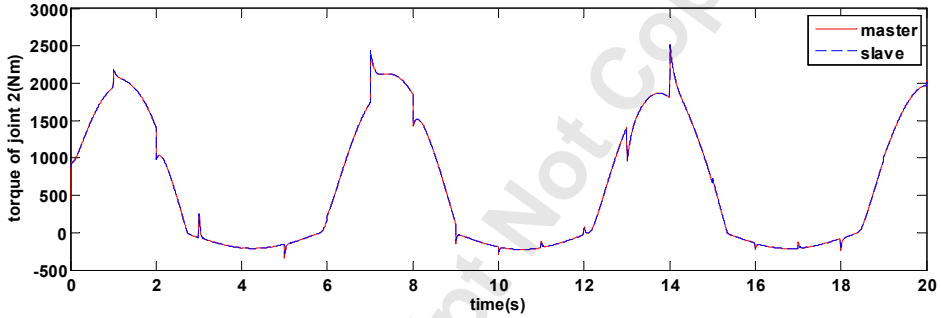


(b)

Fig.10 Torques for the proposed adaptive control with measurement noise. (a) Torque of joint 1. (b) Torque of joint 2.